Selective Electroreduction of CO_2 to Carbon-rich Products by Simple Binary Copper Selenide Electrocatalyst

Apurv Saxena[a], Wipula Liyanage[a], Jahangir Masud[b], Shuben Kapila[a], Manashi Nath[a]*

Supporting Information

Identification and quantification of liquid products

NMR spectroscopy

Liquid products formed during CO_2 electrochemical reduction were analyzed with ^{1}H-NMR. Aliquots were collected at regular intervals as mentioned in the manuscript and 2 µL DMSO (internal standard) and 200 µL D_2O was added to 0.5 ml electrolyte. The NMR experiments were performed on a Bruker 400 MHz NMR spectrometer, using a presaturation sequence to suppress the water signal. NMR spectra of reaction mixture was measured before starting any electrochemical reaction to make sure that there was no impurity in the solution which can lead to false results.

Table S1. Chemical shifts and assignments of peaks from different possible products observed in 1H-NMR spectra after CO_2 reduction.

Observed NMR Values			Products		Standard NMR Values[47]
Chemical Shift	1H Splitting	J coupling	Probed Nucleus	Name	Chemical Shift
8.35			$CHOO^-$	Formate	8.35
3.64	q	7.08	$CH3CH_2OH$	Ethanol	3.64
1.8	s		$CH_3C(=O)O^-$	Acetate	1.8
1.20	t	7.16	CH_3CH_2OH	Ethanol	1.20

Quantification of the products

Liquid products were quantified from NMR spectra by calibrating it with respect to the internal standard and quantifying the identified products.

Gaseous products of CO_2 reduction were collected and transferred to GC using gas-tight syringe. The GC was equipped with thermal conductivity detector (GC- TCD) and Molecular Sieve 5A capillary column. Helium (99.999%) was used as the carrier gas. The GC columns led directly to a TCD detector to quantify hydrogen and carbon monoxide. At ambient conditions, CO_2 was continuously purged through a cathode compartment flow cell at a rate of 20 sccm while a constant potential was applied for designated time. The cell effluent was sampled using 100 µL syringe.

The Faradaic efficiency (FEs) was calculated by measuring the current and using mole percentages quantified through GC-TCD as well as NMR analysis as follows:

Faradaic Efficiency (%) calculation of Products

No. of moles of product = *C*

Total current = I (A)

No. of electrons(moles) required to form certain product = *C* x *n*

N = No. of electrons required to obtain 1 molecule of product.

Charge consumed in forming certain product C_e = *C* x F x *n* [F = Faraday constant, 96485 C mol^{-1}]

The number of electrons required to form a molecule of Ethanol, Acetate, Formate and H_2 are 12, 8, 2 and 2, respectively.

Total charge consumed can be determined using Faraday's laws of electrolysis: $C_T = I \times t$,

Faradaic efficiency of the product = $C_e / C_T \times 100\%$

Following worksheet shows typical calculation of Faradaic efficiency at specific potentials (-0.6 V and -0.9 V vs RHE)

Calculation of the FE of products at -0.6 V vs RHE:

current density mA/cm^2 (1h)= 4 mA/cm^2

Surface Area of the electrode = 2 cm^2

Total current(A) = (current density x Surface Area of the electrode) /1000 = 0.008 A

Total charge consumed C_T = I × t = 0.008 x 3600 = 28.80 C

Table S2: Calculated Faradaic Efficiency along with product concentration obtained at -0.6 V vs RHE.

Products	No. of moles of product(mol)	*n* (number of electrons required to form specific product)	C_e (Charge required to form certain product) (C)	FE = C_e /C_T*100
Hydrogen	2.68E-07	2	0.51	0.18
Ethanol	2.10433E-05	12	24.36	84.00
Acetate	5.72789E-06	8	4.42	15.34
Formate	7.55558E-07	2	0.14	0.48

Calculation of the FE of products at -0.9V vs RHE:

current density mA/cm^2 (1h)= 5.5 mA/cm^2

Surface Area of the electrode = 2 cm^2

Total current(A) = (current density x Surface Area of the electrode) /1000 = 0.01086 A

Total charge consumed $C_T = I \times t = 0.01086 \times 3600 = 39.10$ C

Table S3: Calculated Faradaic Efficiency along with product concentration obtained at -0.9 V vs RHE.

Products	No. of moles of product(mol)	N(number of electrons required to form specific product)	Ce (Charge required to form certain product) (C)	FE = C_e /C_T*100
Hydrogen	1.28E-06	2	0.25	0.64
Ethanol	2.14789E-05	12	24.86	63.58
Acetate	5.3476E-06	8	4.12	10.53
Formate	5.12389E-05	2	9.88	25.25

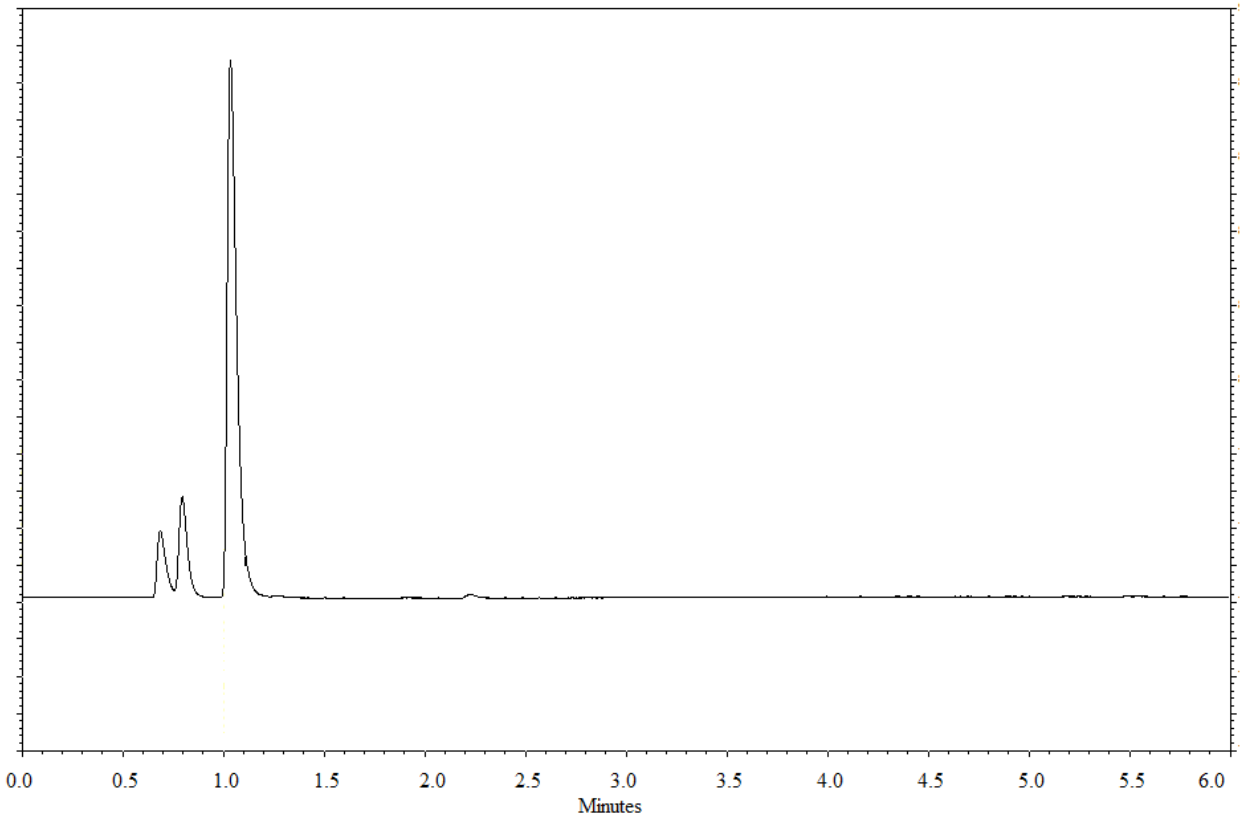

Fig S1. Gas Chromatogram collected at -1.3 V vs RHE from the head-space gas.

Table S4. Faradaic efficiency of the liquid and gas phase products estimated from NMR and GC-TCD respectively at different applied potential with Cu_2Se				
Product	Faradaic Efficiency (%)			
	-0.25 V	- 0.6 V	- 0.9 V	- 1.3 V
H_2	0	0.17	0.63	1.12
Formic Acid	0.4	0.50	25.26	94.2
Acetic Acid	33	15.25	10.54	4.67
Ethanol	66.6	84.06	63.55	0

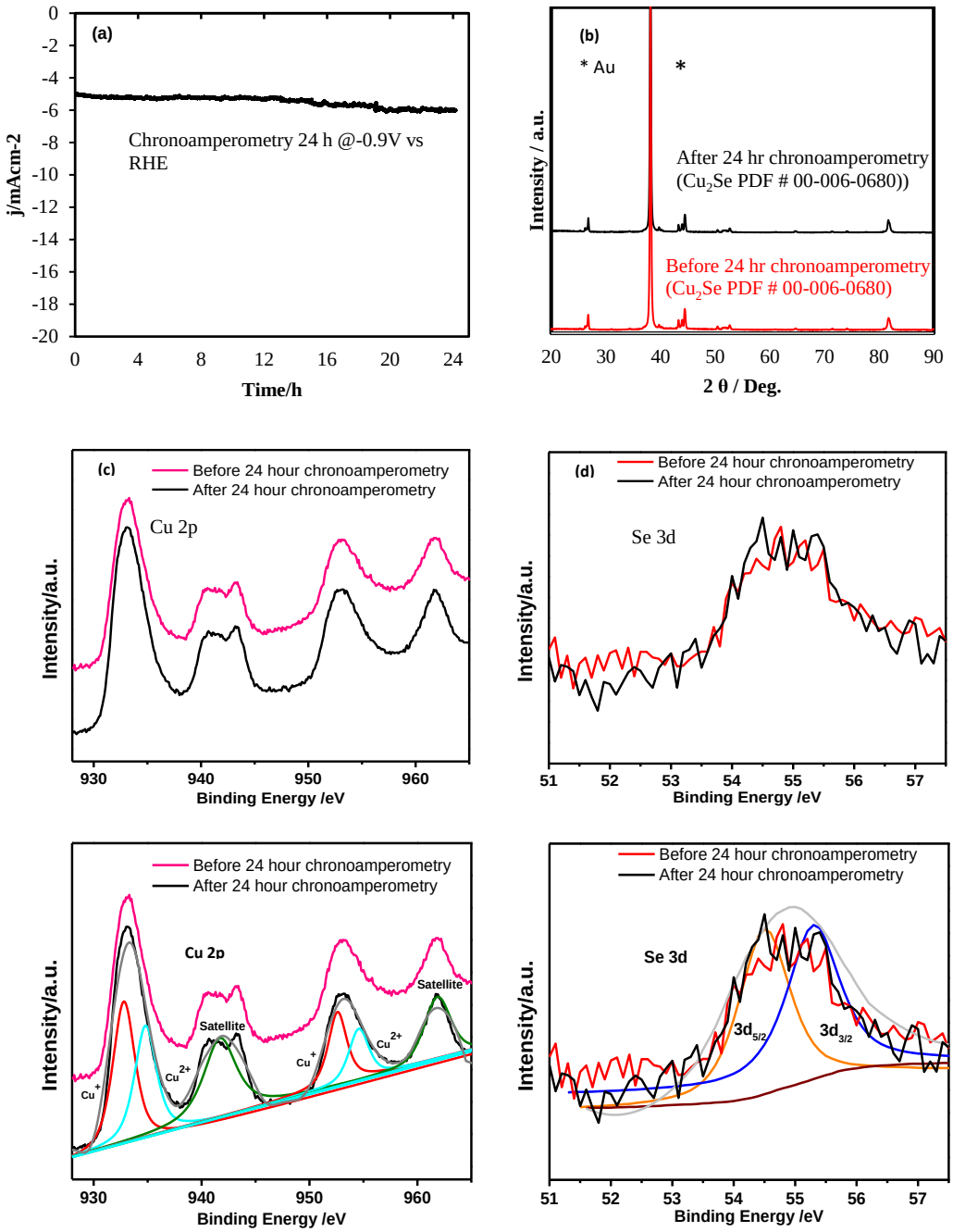

Fig. S2. (a) 24 h of chronoamperometry study at applied potential = -0.9V vs RHE (b) Pxrd spectra of Cu_2Se before and after 24 h of chronoamperometry (c) Cu 2p XPS signal before and after chronoamperometry for 24 h. (d) XPS spectra of Se 3d before and after chronoamperometry study(e) & (f) Deconvoluted Spectra

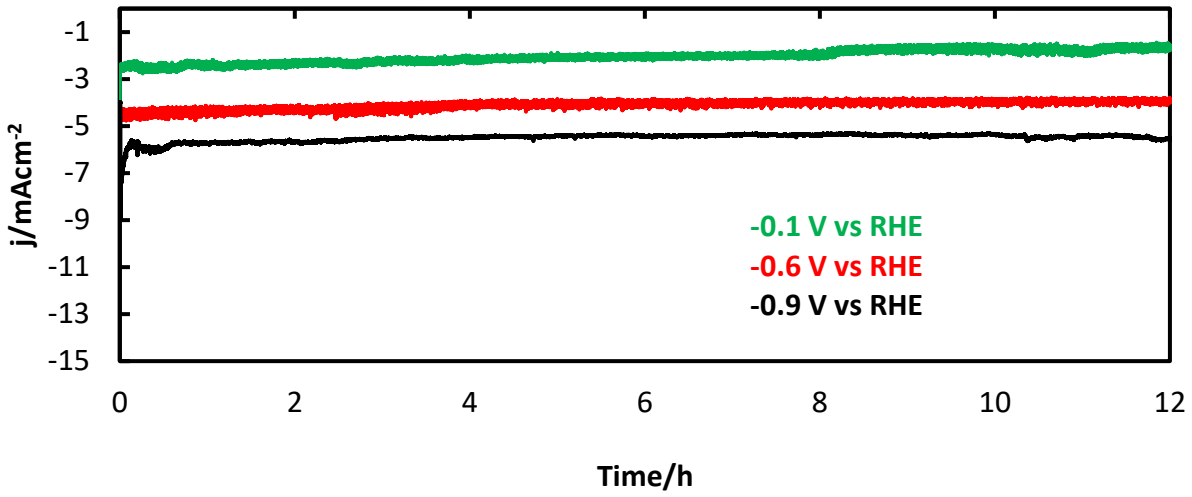

Fig S3. Chronoamperometric stability study for Cu_2Se nanocomposite under continuous CO_2 purging for 12 h held at constant potential (-0.1 V vs RHE, -0.6 V vs RHE, -0.9 V vs RHE)

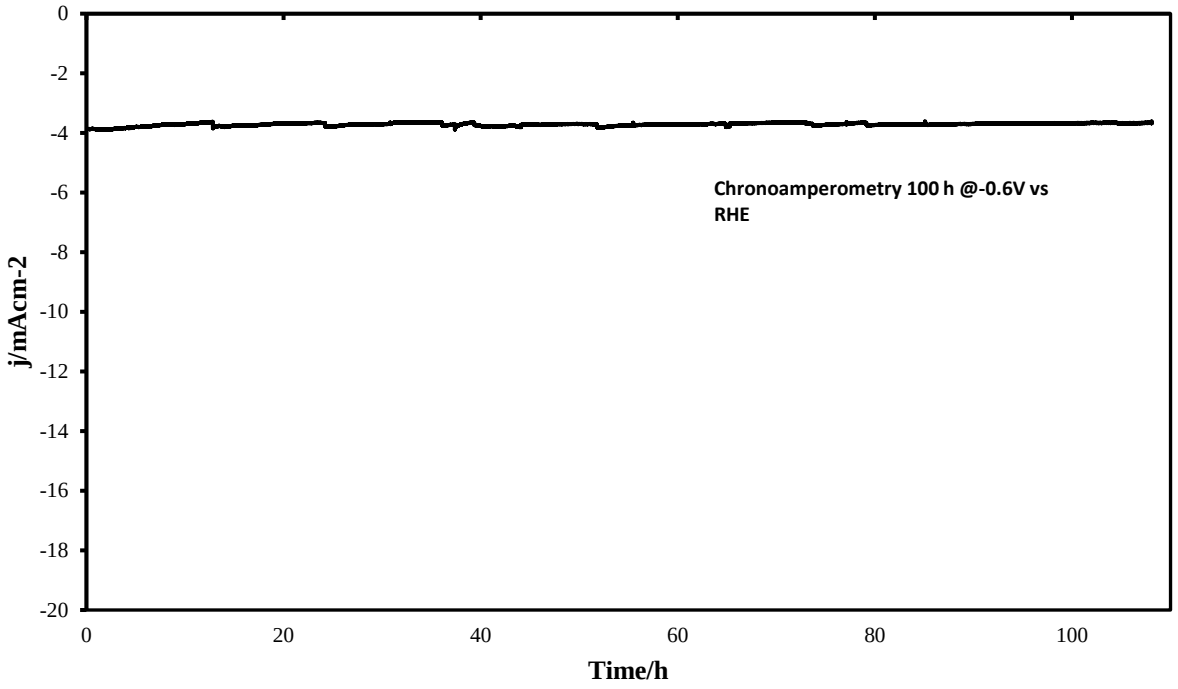

Fig S4. Chronoamperometric stability study for Cu_2Se nanocomposite under continuous CO_2 purging for 100 h held at constant potential (-0.6 V vs RHE)

Computational Setup

The fully periodic plane-wave density functional theory (DFT) calculations were carried out as implemented in Vienna Ab-initio Simulation Package (VASP)[1] with the exchange-correlation functional Perdew−Burke−Ernzerhof (PBE)[2] within the generalized gradient approximation (GGA)[3] implemented with the Projector Augmented Wave function (PAW) method[4] to investigate adsorption energy of CO molecules on the surface of catalyst materials. An energy cutoff limit of 500 eV was applied with the convergence criteria for electronic self-consistent iterations set at 1.0×10^{-6} eV, and the ionic relaxation was carried out by conjugate gradient algorithm until atomic forces of the system were smaller than 0.01eV without any constrains. The Methfessel−Paxton smearing with a value of smearing parameter σ of 0.2 eV was applied to the orbital occupation. The calculations employed 11x11x3 k-point Monkhorst−Pack[5] mesh for Cu and other transition metals along with a 11x8x3 grid for Cu_2Se (220) surface and 11x11x5 grid for Cu_2Se (001) surface for sampling the Brillouin zone. For each species, surface models with a unit cells of 2x2x2 and 2x3x3 with a vacuum region of 15 Å along z-direction were used.

During the calculation of CO adsorption energy, first the free surfaces were relaxed to obtain the energy of the clean surface, E_{clean}, and then CO ions were placed on top of active sites of the catalyst at a distance of ~ 1.80 Å, which is very close to the equilibrium distance of CO on transition metal sites, and let the system to relax to calculate, Esys., the total formation energy of the system. The adsorption energy of CO, E_{ad}, was calculated as $E_{ad} = E_{sys} - E_{clean} - E_{CO}$, in which E_{CO} is the energy of free CO.

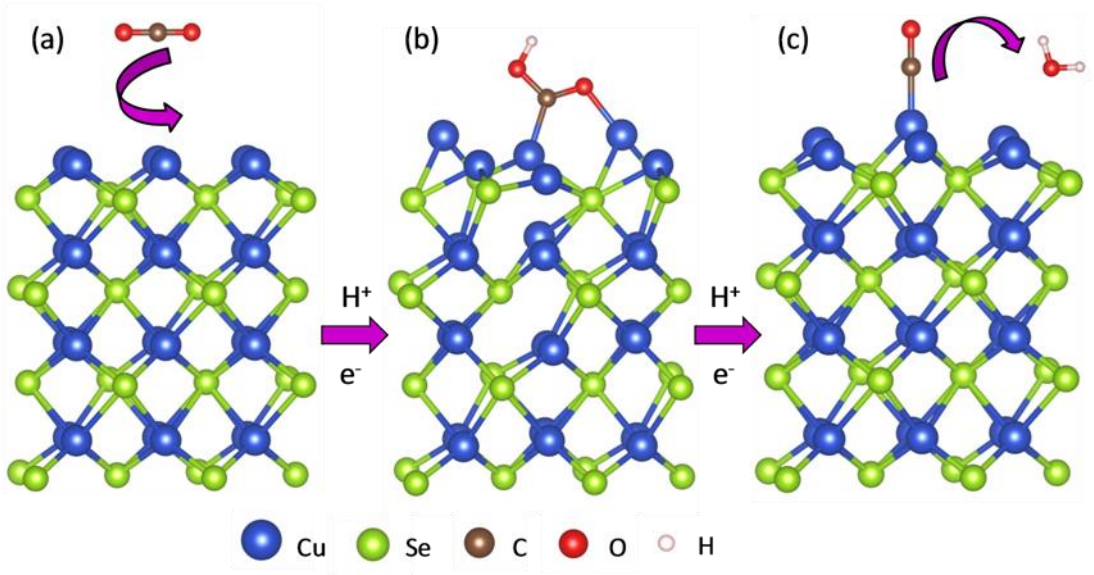

Figure S5. Schematic representation of the elementary reaction steps for the formation of CO on Cu_2Se (001) surface. The simulated *COOH intermediate in (b) shows the formation of a stable configuration on Cu_2Se surface by attaching through C and O atoms to neighboring Cu atoms on the catalyst surface.

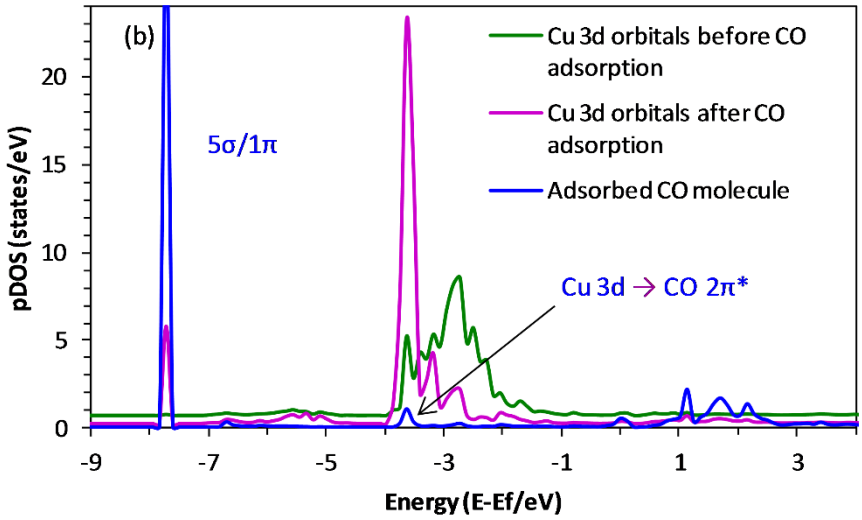

Figure S6. Atom projected partial density of states of the 3d orbitals of a Cu atom on Cu_2Se (001) surface before and after binding with CO molecule. Overall stabilization of Cu 3d orbitals can be seen after binding with a CO molecule. Also, π back bonding feature to the coordinated CO atom has indicated with an arrow.

References

1. Kresse, G., & Furthmüller, J. (1996). Efficient iterative schemes for ab initio total-energy calculations using a plane-wave basis set. Physical review B, 54(16), 11169.

2. Perdew, J. P., Burke, K., & Ernzerhof, M. (1996). D. of Physics, NOL 70118 J. Quantum Theory Group Tulane University. Phys. Rev. Lett, 77, 3865-3868.

3. Perdew, J. P., Chevary, J. A., Vosko, S. H., Jackson, K. A., Pederson, M. R., Singh, D. J., & Fiolhais, C. (1992). Atoms, molecules, solids, and surfaces: Applications of the generalized gradient approximation for exchange and correlation. Physical review B, 46(11), 6671.

4. Blöchl, P. E. (1994). Projector augmented-wave method. Physical review B, 50(24), 17953.

5. Monkhorst, H. J., & Pack, J. D. (1976). Special points for Brillouin-zone integrations. Physical review B, 13(12), 5188.